

Morphological Inversion of Complex Diffusion

V. AT. Nguyen and D. C. Vural*

University of Notre Dame, Department of Physics,
225 Nieuwland Science Hall, Notre Dame, IN 46556 USA

Epidemics, neural cascades, power failures, and many other phenomena can be described by a diffusion process on a network. To identify the causal origins of a spread, it is often necessary to identify the triggering initial node. Here we define a new morphological operator and use it to detect the origin of a diffusive front, given the final state of a complex network. Our method performs better than randomized trials as well as centrality based methods. More importantly, our method is applicable regardless of the specifics of the forward model, and therefore can be applied to a wide range of systems such as identifying the patient zero in an epidemic, pinpointing the neuron that triggers a cascade, identifying the original malfunction that causes a catastrophic infrastructure failure, and inferring the ancestral species from which a heterogeneous population evolves.

A sugar piece placed in tea will erode and eventually dissolve. Given the initial shape of the piece, it is trivial to predict its final distribution. However, the opposite problem of determining the initial state, given a final one is extremely difficult. Problems of the latter kind are referred as ill-posed inverse problems [1–3].

Diffusion taking place on networks, in the forward direction, is well studied. One class of models originally used to describe epidemics is the Susceptible-Infected-Recovered (SIR) model [4, 5]. Variations include SI, SIS, SIRS, etc. Others include more realistic delay conditions, such as an incubation period for the infection [6]. Similar models are used to describe neural cascades [7], traffic jams [8] and infrastructure failures [9].

Accordingly, a successful method of inverting diffusion on complex networks can help identify patient zero in an epidemic outbreak, pinpoint neurons that trigger a cognitive cascades, remedy the parts of the road network that initiate congestion, and determine malfunctions that lead to cascading failures. In the weak selection limit, evolution can be thought as diffusion on a genotype network [10, 11], so diffusion inversion may be used to identify ancestral species.

Here we address the problem of identifying the origin of a diffusive process taking place on a complex network, given the its final state. We refer to the influenced nodes as the candidate set C . Any member of C may be the node from which the diffusion originated. We refer to this node as the seed, s , and to the foward model as M .

Presently, there are two approaches to identify s . The first uses probability marginals using Bayesian methods [12–21]. In some cases, it is possible to sample the state space using Monte Carlo simulations [13]. However, this is only feasible for small networks. Message-passing algorithms can approximate the marginals efficiently [12, 14–16], however these algorithms are model specific: for every M , one must invent new approximations, heuristic assumptions and analytic calculations.

In contrast, the second class of methods works independently of the forward model [14, 17–19]. These presuppose that s should be approximately equidistant to

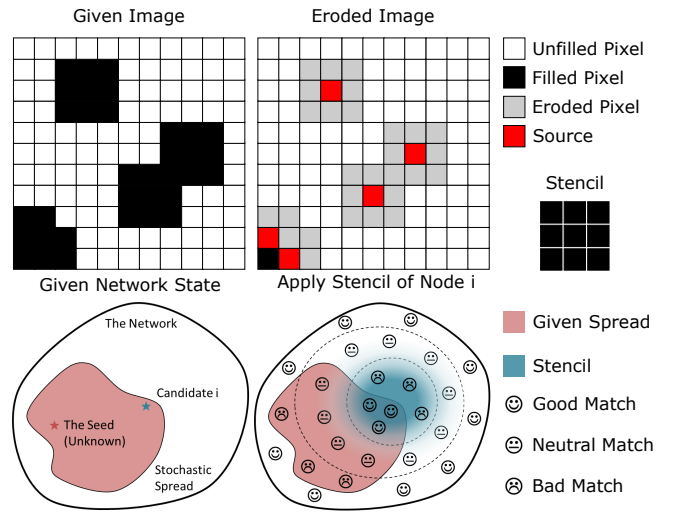


FIG. 1. Example of classical erosion (top) and our generalization (bottom). Top: The structuring element (“stencil”) is placed on individual pixels whose neighborhoods are checked for a match/mismatch. If there is a mismatch, the pixel is deleted. In the end, shapes loose outer layers. Bottom Left: the network and candidate (red) set is given while the seed (red star) is unknown. Bottom Right: the erosion stencil (blue gradient) for candidate i (blue star) is applied over the network. Smiley faces show the locations where the stencil matches the given network state, neutral faces show locations of high variability, and sad faces show regions where the stencil does not match the candidate set.

all other nodes in C , and therefore, nodes with high centrality values should have a higher likelihood of being s . This assumption breaks down if the spread reaches “boundaries”, or if the spread self-interacts (i.e. if the network contains many loops rather than being a tree).

Here we present a method that can determine the origin of a diffusive process taking place on a complex network, regardless of what the diffusion model is, without the drawbacks of centrality based methods. We take as inputs the network structure, the candidate set C , and the forward model M . In return, we output a list of

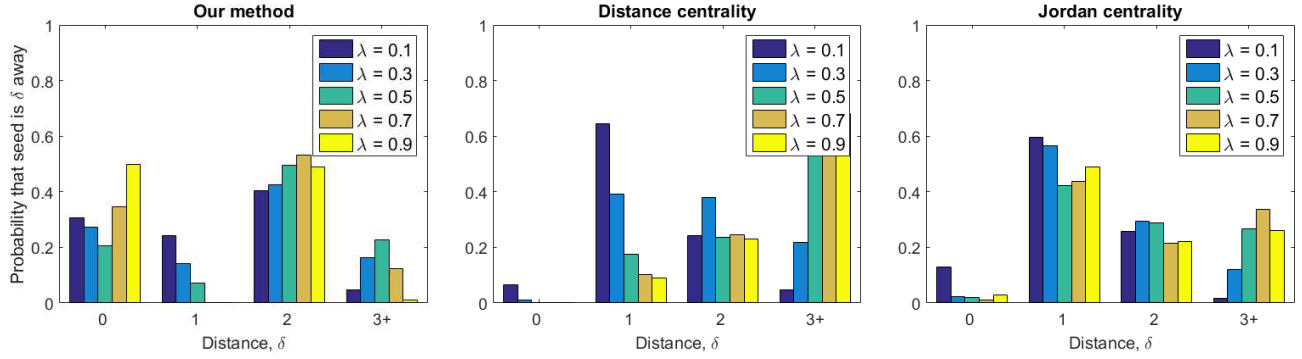


FIG. 2. Error distance δ for the protein interaction network ($n = 3744$ and $m = 7749$) using our method/distance centrality/Jordan centrality (left to right). δ is the distance between the top candidate and the true origin.

nodes, ordered according to the likelihood of being the seed s . We emphasize that our method has no free parameters and is applicable to any M , including both deterministic and stochastic forward models.

To evaluate our success, we perform simulations in the forward direction using 4 types of forward models on 3 different graph topologies. We then inverted the final state, and determined how often our guess is the true seed. We also measured the error distance, i.e the distance of our guess from the true seed.

The forward models we explored are Susceptible-Infected (SI) epidemic model with uniform propagation probability between neighboring nodes; an information cascade (IC) model which propagates the diffusion like the SI model but with an additional cascade effect based on the fraction of infected neighbors [22]; a collective behavior (CB) model based on the notion that social behavior is determined by threshold for when the benefit of an action is greater than its cost [23]; a heterogeneous SI model where the propagation probability has a directional bias (DB) based on spatial positions of the nodes.

The network topologies on which we evaluate our model consist of a real power grid (GRID) network of the western states of the USA [24], a real protein (PROT) interaction network of *C. elegans* [25], and a synthetic scale free (SCLF) network based on the power grid network.

The spread time was selected so that the number of affected nodes were as large as possible without the diffusion process filling the entire network. We did not explore cases for low propagation probability and large spreads in order to maintain a uniform time-scale for all models.

Generalized Morphological Operators. The principle behind our method can be best described by the language of mathematical morphology pioneered by Minkowski, Matheron, Serra and others [26–28]. A morphological operator modifies every point in a set (e.g. an image) according to the spatial arrangement of neighboring points. A stencil, called the “structuring element”, with a predefined shape is placed on individual points,

and if the surroundings of the point match (or not match) the shape of the stencil, then the point is modified. One particular operator, “erosion”, is important for our purpose. Erosion, deletes all points whose surroundings mismatch the structuring element. Since a mismatch would typically happen near the boundaries of a shape, the erosion filter ends up rounding up and thinning down all shapes. This is the qualitative behavior we need in order to get rid of the peripheral nodes of C and reach its core.

To suit our specific purpose, we define a new morphological operator analogous to erosion, but with three important differences (Figure 1). First, our structuring element is not fixed, but changes according to where it is placed on the network. Furthermore, our structuring element does not have sharp edges, but is fuzzy. To be precise, we take the structuring element, when placed on i , to be $P(j|i)$, which we compute numerically.

Secondly, the comparison of the structuring element and the surrounding nodes of i is not binary, but weighted. This is because mismatches of deterministic events (e.g. $P(i|j) \sim 0$ or 1) matter more than random events ($P(i|j) \sim 0.5$). To be precise we weight every node mismatch with a factor inversely proportional to the binary entropy $H_b(P(j|i))$.

Thirdly, the final effect of processing a node with a structuring element is not simply deleting or keeping. Instead, this too is fuzzy. In the end, upon applying our morphological operator to the network once, we expect the least eroded node to be the seed.

Our algorithm generates an ordered list of candidate seeds based on how much they are eroded. The best case scenario is when the true origin is located at the top of this list. Fig. 1 schematically shows an evaluation of the match between an erosion stencil and the given network state along with an example of classical image erosion. The mathematical details of our morphological operator is explained in the Method section and *Suppl. Mat.*

Results. We plot the distance between the true origin and the best guess of our algorithm and compare these

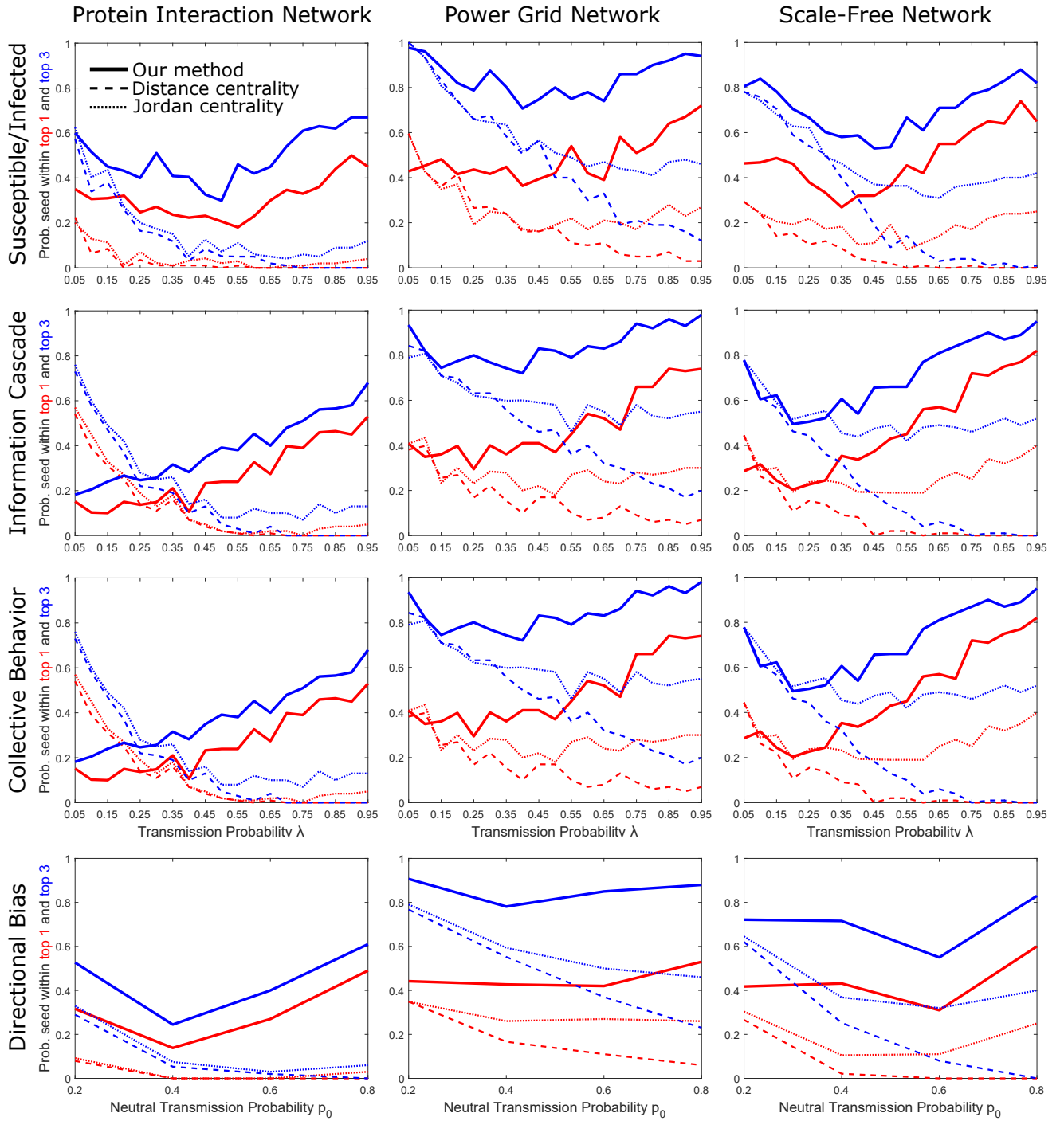


FIG. 3. Performance on different networks and models as a function of the transmission probability λ , for $T = 5$. The protein interaction network ($n = 3744, m = 7749$), power grid network ($n = 4941, m = 6594$), and scale-free network ($n = 4941, m = 6601$) are shown from left to right. The four dynamic models are shown in each row. Note the difference between the uniform transmission probability, λ , and the neutral transmission probability, p_0 . Our performance (red/blue solid curves) is almost always better than centrality based methods (dashed and dotted lines of the same color)

results to other non-model-specific methods. Overall, our algorithm performs much better than distance and Jordan centrality on the same graph type and size. Fig. 2 shows, in a representative model and network topology, that our first guess is almost always within two hops away from the true seed. This is the case for all other models and topologies (cf. *Supp. Mat*).

Figure 3 shows how often the true seed is our top guess and how often it is within our top three guesses. The bold solid lines show the performance of our algorithm, while the dashed and dotted lines show the performance of distance centrality and Jordan centrality based methods. Our success rates are far above the dashed and dotted curves of the same color, with the only exception of the low λ regime of the IC model.

On average the radius of C is $\langle r \rangle = T\lambda$ nodes. As $\lambda \rightarrow 0$, there are few nodes to pick from, and thus centrality based methods, including just randomly selecting a node from C , gives similarly high success rates as our method. As λ is increased however, the difference between our method and others increase significantly. The difference in success is maximal when the number of affected nodes become maximum, at $\lambda \rightarrow 1$. Across all forward models, we have least success when the spread probability $\lambda \sim 0.5$, the regime with the highest number of possible states due to the high variability in the stochastic process. This variability causes the calculated average stencil to very rarely match a given diffusion state.

In general, stochastic dynamics on networks will be defined in terms of local properties rather than global ones. To this extent we explored two main variations to a local property, i.e. models in which fractional versus absolute number of affected neighbors determining the spread probability. We have also shown that our algorithm performs well for non-uniform and directionally-biased diffusion. Hence, we have explored, nearly to full extent, the inversion of two state diffusion processes on complex networks.

Our algorithm is a general method for determining the source of diffusion dynamics on complex networks. It requires knowing the dynamic law as well as the states of all nodes at some final time. The performance of our algorithm may be improved by degeneralizing the scoring function to accommodate particularities of a forward model. We also note that there are many aspects of the problem we have not yet considered, such as cases of incomplete or noisy information, dynamics of multi-state diffusion, and even multi-source diffusion [12, 13, 15, 16, 20, 21].

It should be possible to extend our method for multi-source diffusion and/or multi-state diffusion. In the case of multi-source, one could generate a scoring metric which is non-symmetric against the diffusion state. In other words, the scoring could prioritize matching the diffusion state rather than the base state. In the case of multi-state diffusion, one could introduce a transition

matrix for the states where the elements of this matrix represents how easy/difficult it is to transition from one state to another. This matrix must be embedded into the scoring metric such that mismatches in state are weighted by the elements of this matrix.

We conclude our discussion with our limitations. As usual, there is a trade off between accuracy and generality. Our method should not be expected to perform better than methods that are custom tailored to specific models. By studying the specific dynamics, one can generate additional constraints and properties of the dynamics such as tree-topology, exact analytical solutions, conservation laws, etc, that might aid in inversion [17, 19]. Furthermore, the performance of our algorithm can be enhanced by extending what we have done with 2-body correlations to n -body correlations or time dependent correlations to calculate path integrals based on Bayesian inference (e.g. [12] for one specific model). However, generalizing such approaches for *any* forward model and *any* network topology is offset by the huge number of simulations required to resolve the correlations to within a useful error margin, and will be very costly.

Models. We used a protein-protein interaction network [25], a power grid network [24], and a synthetic scale-free network to evaluate our method. The SI model is defined by the probability $p_{ij} = \lambda A_{ij} I_j$ of a process spreading from j to i , Where A_{ij} is one when nodes i and j are connected by an edge and zero otherwise and I_j is one if node j is infected and zero otherwise. Which simplifies to j infecting i with probability $\lambda = [0.05, 0.1, \dots, 0.95]$ only if the two nodes are adjacent and j is infected. The IC model cascades the information spread based on a critical fraction of neighbors:

$$p_{ij} = \begin{cases} 1 & \sum_j A_{ij} (I_j - \nu) \geq 0 \\ \lambda A_{ij} I_j & \sum_j A_{ij} (I_j - \nu) < 0 \end{cases} \quad (1)$$

The CB model spreads the adaptation of a social behavior when the number of neighbors who have adopted the behavior reaches a threshold:

$$p_{ij} = \begin{cases} 1 & \sum_j A_{ij} I_j \geq \mu \\ \lambda A_{ij} I_j & \sum_j A_{ij} I_j < \mu \end{cases} \quad (2)$$

We implemented these models using $\mu = 2$ and $\nu = 0.5$. The DB model uses heterogeneous diffusion probabilities $p_{ij} = B_{ij} I_j$, where $B_{ij} = A_{ij} (p_0 + \delta p \cos(\vec{d}_{ij} \cdot \vec{b}))$. The DB model is generated by first randomizing the three dimensional positions for all nodes placed inside a unitary volume and then calculating the unit displacement vector, \vec{d}_{ij} , between adjacent nodes. We then picked a unit bias vector, \vec{b} , pointing towards one of the corners of the volume and generated the weighted adjacency matrix B_{ij} based on a neutral transmission probability $p_0 = [0.2, 0.4, 0.6, 0.8]$ and range $\delta p = 0.15$.

Method. The structuring elements are generated by directly sampling the states of the network model. For

each model, we applied the selected diffusion dynamics 500 times for every node in the network and recorded the results. The structuring element, $P(i|j)$, is calculated based on the normalized frequency of finding node i affected given that node j was the origin. We note that we have tried increasing the sample size up to 10^4 and found very similar but slightly better results.

The idea behind our morphological filter is to determine which stencil has the best match with the given diffusion state. The likelihood of a node being the origin node is proportional to the similarity between its stencil and the diffusion state. However, there are many ways to measure the similarity between a probability vector and a binary vector. We sampled the performance of different scoring metrics such as log-likelihood (under independent 3-body correlations), information surprisal, Pi-cards distance. The results shown in this paper are based on the an information theoretical metric which we found to work best, $S_i = \sum_j |I_j - P(j|i)|/H_b(P(j|i))$, where, $H_b(x) = x \log_2 x + (1-x) \log_2(1-x)$. S_i measures the mismatch between the stencil and diffusion state weighted by the binary entropy as the weight. This weight will diminish the value of nodes with high variability ($p \approx 0.5$) in comparison to nodes with low variability ($p \approx 0$ or $p \approx 1$). If the probability that a node is affected is very high or very low but the state of the spread gives the opposite result, then it is unlikely that this stencil matches with the spread and therefore is given a higher (worse) score. On the other hand, if there is a high variability event, such as a coin flip, we are not very surprised or interested in the result of a single trial (we only have one diffusion state for comparison). We sorted the scores in ascending order and the results shown in this paper is based on the lowest scoring nodes. Numerically, the inverse binary entropy can result in a division by zero, and therefore instead of directly using $P(j|i)$ we used $P(j|i) + \epsilon$. Where $\epsilon = 10^{-20}$ is small enough to not change the results of the standard deviation and instead provide an upper bound for a highly unexpected mismatch.

We thank Fatos Yarman Vural for her insights. This material is based upon work supported by the Defense Advanced Research Projects Agency, HR0011-16-C-0062.

* dvural@nd.edu

- [1] Tarantola A (2005) *Inverse problem theory and methods for model parameter estimation*. (SIAM, Philadelphia).
- [2] Soussen C, Idier J, Brie D, Duan J (2011) From Bernoulli-Gaussian Deconvolution to Sparse Signal Restoration. *IEEE Trans Signal Process* 59(10):4572-4584.
- [3] Ruiz P, Zhou Xu, Mateos J, Molina R, Katsaggelos AK (2015). Variational Bayesian Blind Image Deconvolution: A review. *Digit Signal Process* 47:116-127.
- [4] Keeling MJ, Eames KT (2005) Networks and epidemic

models. *J R Soc Interface* 2(4):295-307.

- [5] Kermack WO, McKendrick AG (1927) A contribution to the mathematical theory of epidemics. *Proc Math Phys Eng Sci Aug* 1 (Vol. 115, No. 772, pp. 700-721).
- [6] Zhen J, Ma Z, Han M (2006) Global stability of an SIRS epidemic model with delays. *Acta Mathematica Scientia* 26(2):291-306.
- [7] Wang J, Lu JG (2008) Global exponential stability of fuzzy cellular neural networks with delays and reaction-diffusion terms. *Chaos Solitons Fractals* 38(3):878-85.
- [8] Kurtze DA, Hong DC (1995) Traffic jams, granular flow, and soliton selection. *Phys Rev E* 52(1):218.
- [9] Arianos S, Bompard E, Carbone A, Xue F (2009) Power grid vulnerability: A complex network approach. *Chaos: An Interdisciplinary Journal of Nonlinear Science* 19(1):013119.
- [10] Huynen, Martijn A (1996) Exploring phenotype space through neutral evolution. *J Mol Evol* 43.3:165-169.
- [11] Wilke, Claus O (2001) Adaptive evolution on neutral networks. *Bull Math Biol* 63.4:715-730.
- [12] Altarelli F, Braunstein A, DallAsta L, Lage-Castellanos A, Zecchina R (2014) Bayesian inference of epidemics on networks via belief propagation. *Phys Rev Lett* 112(11):118701.
- [13] Antulov-Fantulin N, Lancic A, Smuc T, Stefancic H, Sikic M (2015) Identification of Patient Zero in Static and Temporal Networks: Robustness and Limitations. *Phys Rev Lett* 114(24):248701.
- [14] Shah D, Zaman T (2010). Detecting sources of computer viruses in networks: theory and experiment. *ACM SIGMETRICS Performance Evaluation Review* 38(1):203-214.
- [15] Altarelli F, Braunstein A, DallAsta L, Ingrosso A, Zecchina R (2014) The patient-zero problem with noisy observations. *J Stat Mech P10016*.
- [16] Lokhov AY, Mzard M, Ohta H, Zdeborov L (2014) Inferring the origin of an epidemic with a dynamic message-passing algorithm. *Phys Rev E* 90(1):012801.
- [17] Dong W, Zhang W, Tan CW (2013) Rooting out the rumor culprit from suspects. *IEEE International Symposium Information Theory Proceedings* 2671-2675.
- [18] Shah D, Zaman T (2012) Rumor centrality: a universal source detector. *ACM SIGMETRICS Performance Evaluation Review* 40(1):199-210.
- [19] Shah D, Zaman T (2011) Rumors in a network: who's the culprit?. *IEEE Trans Inf Theory* 57(8):5163-5181.
- [20] Hu W, Tay WP, Harilal A, Xiao G (2015) Network infection source identification under the SIRI model. *Proc IEEE Int Conf Acoust Speech Signal Process* 1712-1716.
- [21] Jiang J, Wen S, Yu S, Xiang Y, Zhou W (2016) Rumor Source Identification in Social Networks with Time-varying Topology. *IEEE Trans Dependable Secure Comput* 10.1109/TDSC.2016.2522436
- [22] Watts DJ. (2002) A simple model of global cascades on random networks. *PNAS* Apr 30;99(9):5766-71.
- [23] Granovetter M (1978) Threshold models of collective behavior. *Am. J. Sociol.* May 1:1420-43.
- [24] Watts DJ, Strogatz S (1998). Collective dynamics of 'small-world' networks. *Nature* 393(6684):440-442.
- [25] Stark C et al. (2005). BioGRID: a general repository for interaction datasets. *Nucleic Acids Res* 34(suppl 1):D535-D539.
- [26] Serra, Jean. Image analysis and mathematical morphology. Academic Press, Inc., 1983.

- [27] Haralick RM, Sternberg SR, Zhuang X (1987) Image analysis using mathematical morphology. *IEEE Trans Pattern Anal Mach Intell* 5:32-50.
- [28] Ghosh PK (1988) A mathematical model for shape description using Minkowski operators. *Comput Vis Graph Image Process* 44(3):239-69.